Shaft cooling and the influence on the electromagnetic performance of traction motors

Y. Gai[1], M. Kimiabeigi[1], J. D. Widmer[1], Y. C. Chong [2], J. Goss[2], U. SanAndres[2], D. A. Staton[2]
[1]Affiliation 1; Newcastle University, Newcastle Upon Tyne, NE17RU, U.K y.gai1@ncl.ac.uk
[2]Affiliation 2; Motor Design Ltd., Ellesmere, SY12 0EG, U.K, eddie.chong@motor-design.com

***Abstract*— This paper addresses the heat transfer coefficient associated with a shaft-cooling of traction motors. In such shaft-cooling systems, the 50-50 ethylene glycol-water is made to flow through the shaft hole in order to cool the machine. The heat transfer coefficient is estimated using a CFD (computational fluid dynamics) method, where the effect of rotational velocity as well as liquid flow rate have been accounted for. The results from two different turbulence models were compared. As a result of the simulations, it is concluded that the rotational speed can significantly increase the convective heat transfer in the shaft hole above the stationary condition. Finally, the benefits of implementing a shaft-cooling to an existing ferrite magnet traction motor, in terms of continuous torque capability, is described.**

Keywords— CFD, Traction Motors, Heat Transfer, Shaft Cooling.

Introduction

An electrical machine design must fulfil targets such as small packaging, high torque and high power density in order to be competitive on the market. When creating such machines, the designer is inevitably required to consider the problem from a multi-physics perspective. The latter would include looking at electromagnetic, thermal and structural issues in order to meet any particular customer requirements [1-3]. With regards to thermal analysis, the heat is generated by the electromagnetic losses created, mainly, in the windings and laminations. On the other hand, both the demagnetization of the magnets and the insulation aging may occur due to the temperature rise within the machine.

Due to the airgap acting as an excellent insulation around the rotor, an inner rotor is, often, associated with a poor heat transfer coefficient as a result of which the electromagnetic performance of the motor is compromised. Forced air cooling with a shaft-mounted fan or an extra blower have investigated by many authors for totally enclosed fan-cooled (TEFC) [4-6] machines and open drip proof (ODP) enclosure machines [7, 8]. The sufficient air flow is created to remove heat from the interior parts of the machine. This approach, however, the cooing capabilities is not afford for the high speed, high power density. In order to increase the heat dissipation rate without extra devices. The special fluid is used in some applications. The machine is totally flooded in the oil [9, 10]. The rotor, stator surfaces are directly flushed by a coolant. The enclosed air is replaced by a high conductivity medium. The heat transfer coefficient has an incensement. But this is not an economical and practical methods. The properties of liquid coolant has a very high requirement. The oil friction losses in the airgap is also an issue. Besides, being a rotary part, a direct liquid cooling of the rotor is difficult to manufactrue. Threby, a shaft-cooling is an indirect way to reduce the rotor temperature.In [11], the coolant is introduced into a hollow rotor shaft which is connected to a stationary injection tube. The stationary tube is fixed to a flange that is attached to the stator housing. The coolant is introduced into the system via a coupling connected to a stationary inner tube where it is driven back between the injection tube and the hollow rotor. Reference [12] contains a heat pipe that is inserted through the shaft hole. The heat is dissipated by the metallic plate that is located in the extension of the shaft.

The heat transfer characteristics of a rotating system are rather complex, due to the existence of a secondary flow. It is because not only the Centrifugal force, but also the Coriolis force play a significant roles, while the boundary layer flow may be three-dimensional. As a result, the heat transfer for a rotating duct cannot be estimated using the same correlations applied for a stationary case. Data for convective heat in a rotating cylinder with an axil flow around its axis systems still very inadequate. Reference [13]is one of the first authors to measure the convection heat transfer in flow through rotating ducts. A good understanding of the flow mechanism in a rotating shaft provide a special value in the explanation of heat transfer behavior. Reference [14]conducts both experimentally and theoretically on a hydrodynamically and thermally fully-developed laminar. The laminar flow becomes turbulent due to a destabilizing effect of rotation and enhance the heat transfer coefficient. Free convection vortices, which appear in a heated pipe, disappear as the rotational velocity increases. In [15], experiment is used to examine that the most pronounced effect of rotation on the heat transfer is observed in the transition from laminar to turbulent flow region. Rotation produced less effects in the laminar flow region and no measurable effects once the flow became fully turbulent. However, the literature only can be applied in a relatively limited range. It is difficult to find out a general correlations or trends for convection heat transfer on a rotating system.

Due to the complicated turbulent phenomenon inside of rotating flow, an analytical derivation is not feasible. The convective heat transfer coefficient for the rotating flow which depends highly on the flow phenomenon and cannot be calculated analytically. The numerical simulation method provides a possible way of computing convective heat transfer coefficients of complicated turbulent flow flied. In [16] , the stator convective heat transfer of radial and axial

ventilation holes is investigated for an air-cooled axial-flux permanent magnet machines. CFD model is used to study the effect of the inlet configuration on cooling performance. The convective heat transfer coefficient on the end windings is derived by CFD simulation and compared to measurement in [17].

In this paper, a hollow shaft indirect rotor cooling is investigated. The study of fluid flow and heat transfer in rotating shaft is presented based on computational fluid dynamics (CFD). The results of various turbulence models and rotating speed are compared. The interest in this subject results mainly from the need to determine heat transfer between the surfaces of shaft and the components of rotating machines. In order to indicate some important heat transfer characteristic of rotating shaft, the brief survey of various inlet velocity is researched. Finally, a shaft-cooling is implemented on an existing ferrite magnet traction motor. The maximum rotor and stator are compared between with and without shaft-cooling system. Besides, the continuous torque capability is described.

Computational fluid dynamics

1. The hollow shaft model and Mesh definition

Instead of a whole machines, only a three dimension of hollow shaft was modelled to simulate flow dynamic and heat transfer in the Starccm+. The active part of shaft is 180mm in long with 5.5 mm thick wall. The extra parts for both side were built as well without heat source. The inside diameter of shaft is 24mm which is full of coolant. **Error! Reference source not found.**shows a symmetry cross section of model. The white is for solid region, which only the heat equation has to be solved. Whereas for the fluid regions that is represented by blue domain, also the mass transport needs to be considered. 50-50 ethylene glycol-water and aluminium are represented the properties of coolant and shaft in the CFD model, respectively.

Fig. 1 .Mesh of cross section plane (Grey – Solid, Blue – Liquid)

A conformal mesh which encompasses separate geometry parts without interrupting the continuity of the mesh between solid and fluid domains was created. In a conformal mesh, the perimeter of cell faces that are on the surface of one part, match up exactly with the coincident cell faces on a contacting part. Polyhedral mesher was employed to generate a volume mesh that is composed of polyhedral-shaped cells. Besides, prism layer mesh was used to add prismatic cell layers next to wall boundaries to capture velocity and thermal boundary layers at the wall. The mesh is suitable for heat transfer and swirling flow situations in order to improve the simulation accuracy. The final CFD model consists of 0.36 million computational cells, whereas is about 0.2 million for the solid.

2. Governing Equations and Turbulent model

The rotating reference frame is created to modeling the rotating of shaft and coolant for steady state situation. A constant rotational forces is generated to mimic rotating effects in the rotating domain. Reference[18]found at the entrance of pipe, the rotation causes a destabilization on the flow resulting a swirling flow. It is due to the large shear caused by the rotating pipe wall, in addition to the tangential Reynolds number at 1000 rpm is 14000. So a turbulent model is employed to provide closure of the Reynolds-Averaged Navier-Stokes (RANS) equations in the present study turbulence model.In Reynolds averaging, the solution variables in the instantaneous (exact) Navier-Stokes equations are decomposed into the time-averaged and fluctuating components. The fluctuations of flow velocity generated in the momentum equations are known as Reynolds stress tensor that represent the effects of turbulence.

The coolant is assumed as an incompressible Newtonian fluid with constant fluid properties. Steady-state operation and fully developed turbulent flow were investigated. The continuity equation is used as the transport equation for density and the energy equation is the transport equation for temperature. The effect of gravity is ignored. So the governing differential equations for the Reynolds averaged continuity, Navier Stokes, and energy equations are obtained by

Continuity equation:

$$\frac{\partial U_i}{\partial x_i} = 0 \tag{1}$$

Momentum equation

$$U_j \frac{\partial U_i}{\partial x_j} = -\frac{1}{\rho}\frac{\partial P}{\partial x_j} + \frac{\mu}{\rho}\frac{\partial^2 U_i}{\partial x_j \partial x_j} - \frac{\partial}{\partial x_j}(\overline{u_i u_j}) \tag{2}$$

Energy equation

$$U_j \frac{\partial \Theta}{\partial x_j} = \alpha \frac{\partial^2 \Theta}{\partial x_j \partial x_j} - \frac{\partial}{\partial x_j}(\overline{\theta u_j}) \tag{3}$$

Where μ is fluid dynamic viscosity; ρ is fluid density; U, u are fluid time-averaged and fluctuating Velocity component ; Θ , θ are fluid time-averaged and fluctuating temperature component; α is thermal diffusivity.

Eddy viscosity model is employed to solve the Reynolds stress based on Boussinesq hypothesis. The require closure for the term $\overline{u_i u_j}$ and the scalar transports team $\overline{\theta u_j}$ can be expressed as

$$-\overline{u_i u_j} = \frac{2\mu_t}{\rho} S_{ij}, \tag{4}$$

$$\overline{\theta u_j} = \alpha_t \frac{\partial \Theta}{\partial x_j} \quad (5)$$

Where $S_{ij} = \frac{\partial U_i}{\partial x_j} + \frac{\partial U_j}{\partial x_i}$, $\alpha_t = \frac{\lambda_t}{\rho C_p}$. μ_t, α_t, λ_t are the turbulent fluid dynamic viscosity , thermal diffusivity and Thermal conductivity , respectively.

The turbulence models are basically predicting the unknowns (e.g. Reynolds stresses and turbulent transport of scalar properties) in the turbulent flow field and provide closure to the system of mean flow equations. The accuracy and complexity of RANS turbulence models are associated with the number of additional transport equations that need to be solved along with the RANS flow equations. Consequently, no turbulence model is universal, and a turbulent flow CFD solution is only as good as the appropriateness and validity of the turbulence model used in the calculation [19]. It is important that only the model that has been calibrated with similar flows should be employed, to obtain a physically correct solution caused by the physical accuracy of the turbulence model.

Therefore, Turbulence model is used to solve the Navier-Stokes (RANS) equations. The Realizable *k-ε,* shear stress transport (SST) k-ω model were used to provide closure of the Reynolds-Averaged Navier-Stokes (RANS) equations in the present study. The CFD results obtained using different turbulence models were then compared.

3. Bourndary condition and wall treatment

1kW total heat source was defined in the active part as the machine loss. An uniform power loss distribution was obtained in the CFD model. The outer surface of the shaft are modeled as adiabatic boundary condition. All the heat is dissipated to the coolant through forced convection between shaft inner surfaces and fluids. The pressure for the inlet and outlet model were set 0 Pa and 65 degrees ambient temperature. The inlet coolant flow rate and rotating reference frame speed applied in CFD are list in next section.

The turbulence model is valid only the region where is outside the viscous affected. In the viscous-affected region close to solid walls, the flow field is dominated by shear due to wall friction and damping of turbulent velocity fluctuations perpendicular to the boundary. A wall treatment model was adopted to resolve the viscous-affected region with a high boundary-layer mesh resolution was created with the wall cell $y+ \leq 1$. The all y+ wall treatment was applied for the wall boundary layer between solid and fluid to emulate the accurate prediction of flow and turbulence parameters.

4. Solution Strategy

The governing equations were numerically discretized using a finite volume method to a system of linear algebraic equations were used for numerically discretized. These were solved simultaneously based on the conservation of mass, momentum and turbulence parameters using the second-order upwind discretization scheme.

Analysis

The simulation results for heat transfer, outlet and shaft surface temperature for Realizable *k-ε,* SST k-ω model turbulence models in two different inlet flow rate cases are shown inTable 1.

The value of heat transfer q increase with rotating speed. Due to the coolant adjacent to the shaft wall that is heated, the dense of fluid is less than at the center of the shaft. The centrifugal buoyancy which results from the density variation enhances the temperature exchange between the hot and cold fluid particles. Besides, the secondary flow will occur under the rotation, the cold and dense fluid in the center tend to move radially to the wall due to centrifugal and Coriolis Effect. So rotation changes the flow field in the shaft hole and provides higher convective heat transfer coefficient. The outlet temperature (T_{outlet}) is proportional to the heat transfer, the active part, was determined by (6). So the value of output temperature increase with rotating speed. Due to the increase in convective heat transfer coefficient, the coolant removes more heat when it passes through the shaft hole. The remaining heat of the shaft decreases with rotating speed. As the result, the shaft surface average temperatureT_w is the opposite with speed.

Increasing the inlet flow rate at the low speed has a significant increment on the heat transfer. But when the rotating speed achieve at some point, the inlet flow rate does not have an influence on the heat transfer. But the flow rate is proportional to coolant mass flow rate m , which is the inverse with the outlet temperature. So the case 2 outlet temperature is lower that case 1. The heat transfer of two models are similar. However, the shaft surface average temperature of SST k-ω model is slightly higher than Realizable k-ε.

The reference temperature is obtained by as an average of the inlet (T_{inlet}) and the outlet (T_{outlet})coolant temperatures (7).When inlet temperature is the same, the reference temperature increase is proportional to the speed in all the turbulence models. The calculation of the heat transfer coefficient is shown in (8), where $c_p$is the heat capacity of coolant, A is the shaft active surface part area.

$$q = mc_p(T_{outlet} - T_{inlet}) \quad (6)$$

$$T_{reference} = \frac{T_{inlet} + T_{outlet}}{2} \quad (7)$$

$$h = \frac{q}{A(T_w - T_{reference})} \quad (8)$$

Table 1. The simulated temperature (In degrees Celsius) for Realizable *k-ε,* SST k-ω models after steady state ($\mathbf{T_{inlet}} = \mathbf{65}$℃)

CASE1: 4 liter/ minute flow rate

Speed	Realizable k-ε			Shear Stress Transport (SST) k-ω		
	Heat transfer (w)	Outlet (℃)	Surface (℃)	Heat transfer (w)	Outlet (℃)	Surface (℃)
0rpm	772	68.14	139.71	768	68.12	141.78
8000 rpm	903	68.67	82.54	894	68.62	86.24
15000rpm	922	68.76	77.58	916	68.73	78.86

CASE 2: 8 liter/ minute flow rate

Speed	Realizable k-ε			Shear Stress Transport (SST) k-ω		
	Heat transfer (w)	Outlet (℃)	Surface (℃)	Heat transfer (w)	Outlet (℃)	Surface (℃)
0rpm	830	66.69	108.58	830	66.69	108
8000 rpm	905	66.84	81.14	894	66.82	84.56
15000rpm	922	66.92	75.53	918	66.86	77.16

The heat transfer coefficient for different ratation speeds of Realizable k-ε turbulence model is presented in Fig. 2. Based on the CFD investigation, the CFD results demonstrate that rotation can significantly increase the convective heat transfer in the shaft hole above the stationary condition. The enhancement of heat transfer is mainly due to the increase in convective heat transfer coefficient. The convective heat transfer coefficient of Realizable k-ε turbulence model is slightly higher than SST k-ω model. Rotation changes the flow field in the shaft hole and provides higher convective heat transfer coefficient.

- For 8000rpm, the h is about 5.4 times the h for stationary case,
- For 15,000rpm, the h is about 8.2 times the h for stationary case.

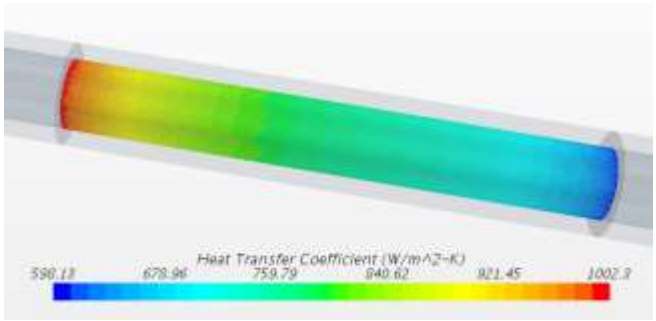

(a)Shaft speed =0 rpm

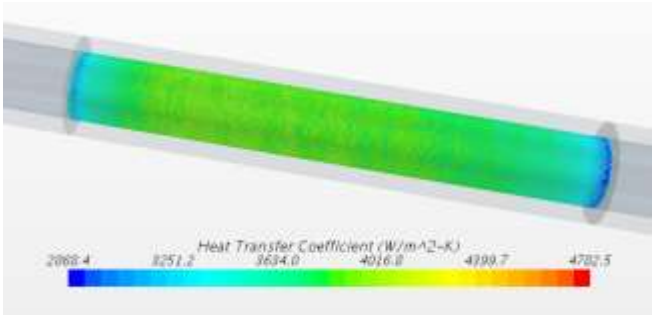

(b)Shaft speed =8000 rpm

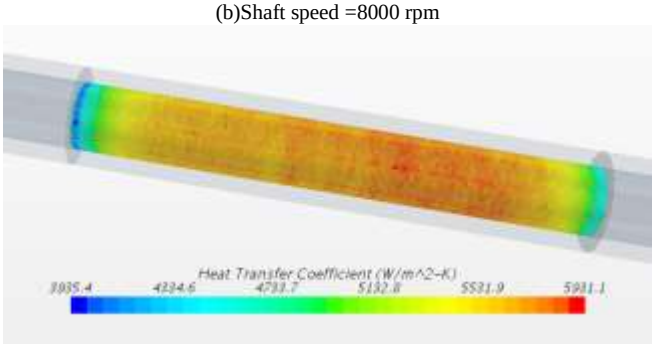

(c)Shaft speed =15000 rpm

Fig. 2 .Heat transfer coefficient in the shaft hole wall at different speed

Keep the same situation, changing the shaft speed to 3000rpm and 30000 rpm. The Fig. 3shows the variation of average heat transfer coefficient with different speed at two different inlet velocity for Realizable k-ε turbulence model. The result of average heat transfer coefficient with speed using different turbulence models are compared. In this case, based on the CFD results, the shaft hole average heat transfer coefficient can be correlated with the rotational speed.

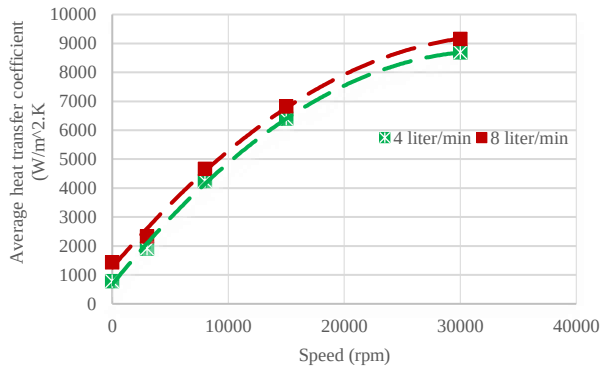

Fig. 3 .The variation of average heat transfer coefficient with speed obtained

Application of the concept to a Ferrite magnet based tarction motor Using the Template

A ferrite magnet motor design, [20], is used to verify the benefits of the shaft-cooling approach on the electromagnetic and thermal performance. An experimental investigation was carried out with 50-50 ethylene glycol-water as a shaft-cooling coolant under various operating conditions. The

variations in the average heat transfer coefficients at the following different shaft speeds is based on Fig. 3 for 4 liter/min.The coupled electromagnetic and thermal analysis is processed by Motor-CAD [21]. A flowchart of couple analysis is illustrated onFig. 4.

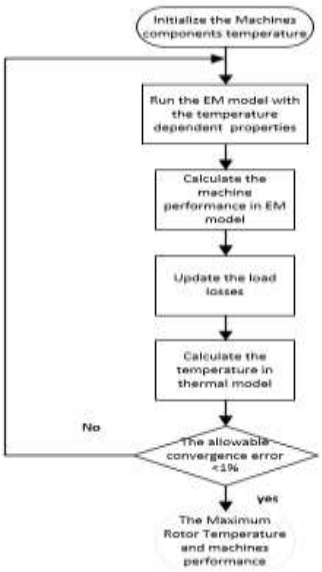

Fig. 4. Flowchart of the coupled analysis

A comparison of the maximum rotor and windings temperature for various speeds with and without the shaft cooling system is shown in Fig. 5. It can be noted that the shaft cooling results in a significant drop of the rotor temperature and a slight decrease in winding. The rotor max temperature has a 50 ℃ decrease at 10000rpm, which corresponds to 15 ℃ at 3000rpm. It is due to an increment at convection heat transfer coefficient at high speed. The similar results can be found in stator temperature as well.

Due to the indirect rotor cooling improve the rotor relatively poor heat dissipation ability. The rotor temperature has been cooled down. As a result, the ferrite magnet working temperature is relative low. Ferrite magnets have a negative temperature coefficient for remanence. So the performance of the ferrite magnets degrades with temperature rise. The continuous torque and power vs speed performance has been presented in Fig.5. It is noted that about 18% output torque increment between with and without shaft cooling.

CONCLUSION

Through a series of CFD calculations, it is concluded that the rotational speed of the shaft can significantly enhance the convective heat transfer coefficient of a shaft cooling system. Based on the findings, the performance of an existing ferrite magnet traction motor has been re-assessed with an added shaft cooling apparatus, where cool down the rotor and stator temperature. A significant improvements in terms of continuous torque and power performance were obtained.

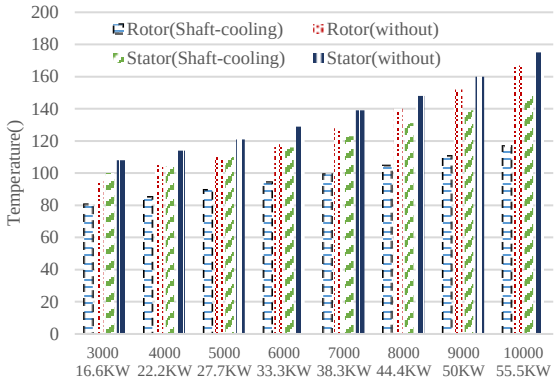

Fig. 5. Maximum stator and rotor temperatures for operating point

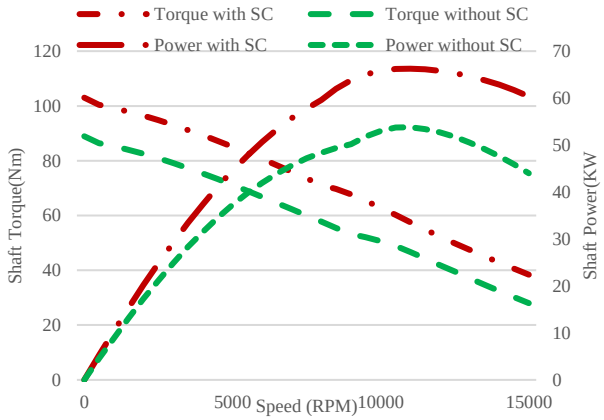

Fig. 6. Torque–speed curve for machines with and without shaft cooling

ACKNOWLEDGMENT

The authors gratefully acknowledge the contributions of Motor Design Ltd. for their work on simulation for the research.

References

1. Miller, T.J.E. *SPEED's Electric Motors*. 2002; Available from: https://www.scribd.com/doc/33998196/Miller-T-J-E-SPEED-s-Electric-Motors.
2. Uzhegov, N., et al., *Multidisciplinary Design Process of a 6-Slot 2-Pole High-Speed Permanent-Magnet Synchronous Machine.* IEEE Transactions on Industrial Electronics, 2016. **63**(2): p. 784-795.
3. Ruoho, S., et al., *Interdependence of Demagnetization, Loading, and Temperature Rise in a Permanent-Magnet Synchronous Motor.* IEEE Transactions on Magnetics, 2010. **46**(3): p. 949-953.
4. Boglietti, A., et al. *Thermal analysis of induction and synchronous reluctance motors.* in *IEEE International Conference on Electric Machines and Drives, 2005.* 2005.
5. Yung, C., *Cool Facts About Cooling Electric Motors: Improvements in Applications That Fall Outside the Normal Operating Conditions.* IEEE Industry Applications Magazine, 2015. **21**(6): p. 47-56.
6. Trigeol, J.F., Y. Bertin, and P. Lagonotte, *Thermal modeling of an induction machine through the association of two numerical approaches.* IEEE Transactions on Energy Conversion, 2006. **21**(2): p. 314-323.

7. Yangsoo, L., H. Song-Yop, and S.K. Kauh, *Thermal analysis of induction motor with forced cooling channels.* IEEE Transactions on Magnetics, 2000. **36**(4): p. 1398-1402.
8. Nakahama, T., et al., *Improved cooling performance of large motors using fans.* IEEE Transactions on Energy Conversion, 2006. **21**(2): p. 324-331.
9. Ponomarev, P., et al. *Thermal modeling of directly-oil-cooled permanent magnet synchronous machine*. in *Electrical Machines (ICEM), 2012 XXth International Conference on*. 2012.
10. Olaiya, M. and N. Buchan. *High power variable frequency generator for large civil aircraft*. in *Electrical Machines and Systems for the More Electric Aircraft (Ref. No. 1999/180), IEE Colloquium on*. 1999.
11. Refaie, A.M.E.-., et al., *Advanced High-Power-Density Interior Permanent Magnet Motor for Traction Applications.* IEEE Transactions on Industry Applications, 2014. **50**(5): p. 3235-3248.
12. Woolmer, T., *ROTOR ASSEMBLY WITH HEAT PIPE COOLING SYSTEM*, in *US patent application*. 2014: United States.
13. KUO, C.Y., et al., *Heat Transfer in Flow Through Rotating Ducts.* Journal of Heat Transfer, 1960. **82**: p. 139-151.
14. Reich, G., B. Weigand, and H. Beer, *Fluid flow and heat transfer in an axially rotating pipe-II. Effect of rotation on laminar pipe flow*. Heat and Mass Transfer, 1989. **32**(3): p. 563-574.
15. Cannon, J.N. and W.M. Kays, *Heat Transfer to a Fluid Flowing Inside a Pipe Rotating About Its Longitudinal Axis.* Journal of Heat Transfer, 1969. **91**(1): p. 135-139.
16. Chong, Y.C., et al., *The Ventilation Effect on Stator Convective Heat Transfer of an Axial-Flux Permanent-Magnet Machine.* IEEE Transactions on Industrial Electronics, 2014. **61**(8): p. 4392-4403.
17. Hettegger, M., et al., *Measurements and Simulations of the Convective Heat Transfer Coefficients on the End Windings of an Electrical Machine.* IEEE Transactions on Industrial Electronics, 2012. **59**(5): p. 2299-2308.
18. Kikuyama, K., M. Murakami, and K. Nishibori, *Development of Three-Dimensional Turbulent Boundary Layer in an Axially Rotating Pipe.* Journal of Fluids Engineering, 1983. **105**(2): p. 154-160.
19. Y.A., C. and J.M. Cimbala, *Fluid Mechanics:Fundamentals and Applications*. New York: McGraw-Hill,2006,pp. 840-853.
20. Kimiabeigi, M., et al., *High-Performance Low-Cost Electric Motor for Electric Vehicles Using Ferrite Magnets.* IEEE Transactions on Industrial Electronics, 2016. **63**(1): p. 113-122.
21. *http://www.motor-design.com*.